A Master/Slave Control of Distributed Energy Resources in Low-Voltage Microgrids

Guido Cavraro, Tommaso Caldognetto, Ruggero Carli, Paolo Tenti[1]

Abstract— **The paper deals with the control of low-voltage microgrids with master/slave architecture. Distributed energy resources (DERs) are interfaced to the grid by means of conventional inverters (slave units), and a microgrid master controller (master unit) governs the interaction between the utility and the microgrid at the point of common coupling with the main grid. The power sharing among the available resources is achieved by the power-based control, a technique which allows to pursue both local (DER level) and global (microgrid level) optimization goals. The paper overviews and analyzes the control algorithm and focuses on how the considered approach can be employed to attain effective modes of operation in microgrids. Simulation results supporting the proposed approach are finally provided and discussed.**

I. INTRODUCTION

Low-voltage microgrids will play a major role in future smart grids [1]. The presence of distributed micro-generation and energy storage owned by end users results in a new paradigm for electrical grids and in a potentially new and vibrant market for technology manufacturers, service providers, energy traders, distributors, and regulatory boards.

The main features of a smart microgrid are highlighted in Fig. 1. Some of the peculiarities of such kind of electrical systems are: high penetration of distributed energy resources (DERs) connected to a low-voltage electrical network, presence of communication links among resources, and presence of a point of coupling with the main grid (i.e., the mains). In this scenario consumers can aggregate to partecipate to the operation of the microgrid by deciding to make available part of their resources, for example, to receive, in exchange, economic benefits.

The power electronic converters interfacing DERs to the grid play here a key role, since they enable extensive power control flexibility, as well as the capability of synergistic use of every available energy resource. Therefore, proper control schemes aiming at coordinating the operation of interface converters will guarantee efficient and sustainable integration of green technologies in low-voltage distribution grids. On the other hand, a high penetration of DERs leads to specific technical challenges that include the management of production intermittencies and energy surplus, and the maximization of the return of investment [2], [3], [4].

In this paper two main issues of low-voltage microgrids are addressed. The first is the regulation of the power flow at the interface between the microgrid and the main grid.

[1] The Authors are with the Department of Information Engineering, University of Padova, Padova, Italy. e-mail: [name].[surname]@dei.unipd.it
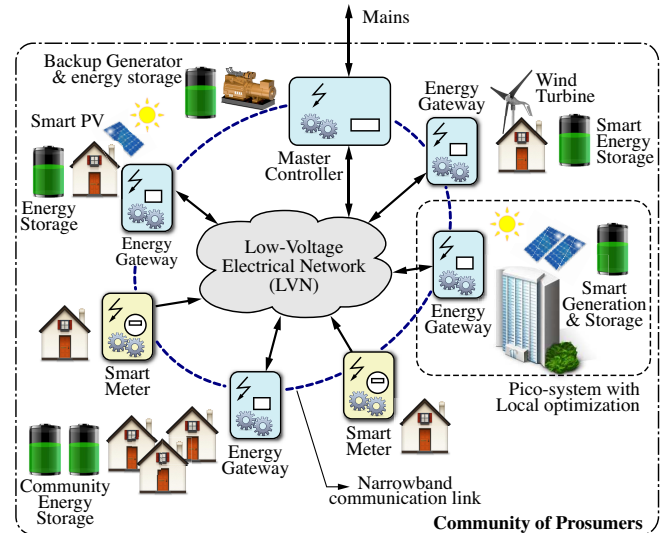
Fig. 1.   Smart microgrid scenario

The second is the management of voltage constraints at grid nodes.

The possibility of regulating the microgrid power absorption is a valuable feature from the point of view of the distribution system operator. In the proposed control scheme this feature, called dispatchability, is attained by exploiting DERs on the basis of their availability in contributing to microgrid's needs. To this end DERs are assumed to be able to communicate—to a centralized controller—their flexibility in participating in the control and to accept, as response, some directives on the required power injection. This allows to define a proper sharing of the load among generators and, in addition, to regulate the power flow at microgrid's PCC. These two objectives usually concern, respectively, the primary and tertiary control level of traditional droop control hierarchies [5], [6], [7].

The second issue addressed herein, that is, the violation of assigned voltage constraint at microgrid nodes, represents an undesirable operating condition that need to be managed in order to preserve the quality of the voltage delivered to the consumers. Besides, uniform voltage profiles along the feeders indicates an adequate utilization of the distribution lines, which is advantageous in terms of reliability and efficiency [8]. This issue is tackled herein by integrating in the centralized control scheme a dynamic overvoltage control technique that allows to coordinately accommodate both the local voltage constraints and the regulation needs at the PCC of the microgrid.

The resulting master/slave control scheme is applied to guide, in a centralized manner, the operation of DERs, while local regulators, embedded in DERs, provide a precise control of active power injection if the measured voltage at the point of connection transcends the nominal operating range.

In the following, in Section II the considered microgrid architecture is introduced. In Section III a model-free power-based control strategy of DERs is introduced and described in details. The stability analysis is provided in Section IV. Finally, Section V reports the results obtained in a realistic simulation scenario. Section VI concludes the paper.

It is worth remarking that the control approach investigated herein was originally proposed in [9], where it is referred to as *power-based control*. In the present paper, a formal and more detailed description of the underlying algorithm, with a different local control rule, is proposed. In addition the stability analysis of the control is introduced and specifically addressed in terms of local and global properties.

II. CYBER-PHYSICAL MODEL OF A SMART MICROGRID ARCHITECTURE

The considered microgrid architecture is shown in Fig. 2. The figure highlights the two layers composing the microgrid structure, namely, the electrical layer and the cybernetic layer. The electrical layer represents the electrical infrastructure, comprising, in particular, the mains, the distributed energy resources, and the electrical distribution network. The cybernetic layer represents the information and communication technology (ICT) infrastructure needed for the monitoring and control of the electrical layer, and comprises the sensors, the computation units, and the communication modules and links.

A. Electrical physical layer

The electrical physical layer can be conveniently modeled as a directed weighted graph $\mathcal{G} = (V, \mathcal{E})$ where V is the set of nodes (i.e., the *buses* of the electric grid) and $\mathcal{E}$ is the set of edges representing the power lines. To each edge e we associate a weight that corresponds to the value of the impendance Z_e of the electric line described by e; specifically $Z_e = R_e + jX_e$, where R_e and X_e are, respectively, the resistive and the inductive component. Because low-voltage grids are addressed herein, we assume that $R_e/X_e >> 1$ for each $e \in \mathcal{E}$, namely, that the interconnection lines are mainly resistive, which is a typical situation in low-voltage grids.

The nodes of the electrical grids can be either *distributed energy resources* or *loads*. A distributed energy resource that can be controlled to contribute to microgrid power needs is herein referred to as an *energy gateway* (EG). The structure of an EG is shown in Fig. 3. In addition to the energy resource, which can be a combination of renewable sources and storage devices, an EG is equipped with a local control unit (LCU) and a power electronic processor (EPP). The LCU collects all the quantities needed to determine the state of the local resources and generates the reference set-point of the power to be injected to the grid. The references
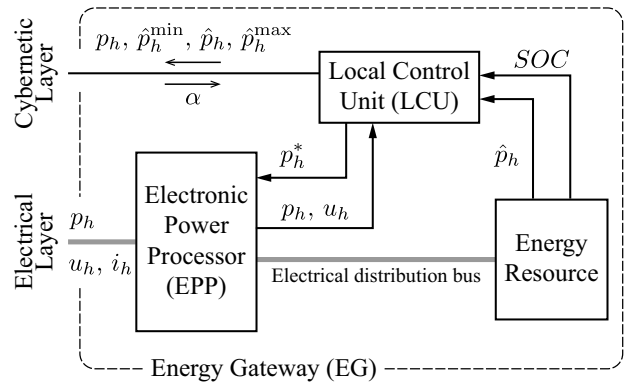

Fig. 3. Structure of an Energy Gateway (EG)

calculated by the local control unit are then actuated by the EPP, which electrically interfaces the energy resources to the grid. The EG interacts through the EPP with the electrical layer, and through the LCU with the cybernetic layer. The figure indicates a set of parameters (e.g., $\hat{p}_h$, α_p) that are related to the state of the EG or of the microgrid; these parameters are detailed in Section III.

We also assume that the microgrid is fed by the utility at the *point of common coupling* (PCC), which is modeled as an ideal voltage source and performs as slack node for the microgrid.

From a mathematical point of view, the electric physical layer can be described by the following variables:

- $u \in \mathbb{C}^n$, where n is the total number of nodes (i.e., $|V| = n$) and where the h-th component of u (i.e., u_h) is the grid voltage at node h;
- $i \in \mathbb{C}^n$, where i_h is the current injected at node h;
- $s = p + iq \in \mathbb{C}^n$, where s_h, p_h, and q_h are, respectively, the complex, the active, and the reactive power injected at node h.

It is convenient to label the variables associated with the PCC with subscript 0. The system variables satisfy the equations:

$$i = Yu \tag{1}$$
$$u_0 = U_N \tag{2}$$
$$u_h \bar{i}_h = p_h + iq_h \qquad h \neq 0, \tag{3}$$

where Y is the bus admittance matrix and U_N denotes the nominal voltage of the grid. It can be shown (see [10]) that there exists a unique symmetric, positive semidefinite matrix $X \in \mathbb{R}^{n \times n}$, called the *Green matrix*, that allows us to express the voltages as a function of the currents via:

$$u = Xi + \mathbf{1}U_N, \tag{4}$$

where $\mathbf{1}$ is the vector collecting all ones.

B. Cyber layer

In this paper a master/slave controller is proposed to supervise the operation of a microgrid. We assume that the *master controller* (MC) is located at the PCC of the microgrid and that the EGs, which are geographically distributed, play as slave units. Both the MC and the EGs are provided with

Data Packet from EGs:
- Max. injectable Power
- Locally Generated Power
- Min. injectable Power
- Injected Power

Master Controller
(**MC**)

Control packet to all EGs

Control Levels

gathering

Σ

Σ

PCC

Mains

broadcasting

ICT Infrastructure

Electrical Infrastructure

Σ

Slave
Agents (**EG**s)

Electrical node
with agent

Electrical node
with no agent

Power-based control
Centralized management of DERs
to fulfill the microgrid power needs
Actors: MC and EGs

Local control
Local optimization of energy
resources and local power quality
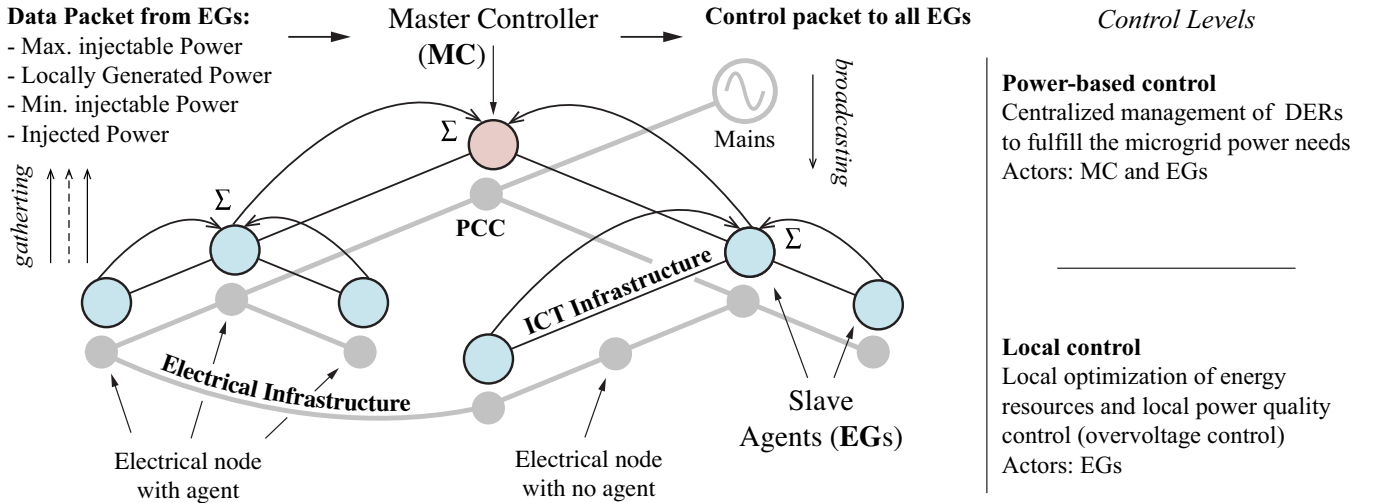control (overvoltage control)
Actors: EGs

Fig. 2.   The considered master/slave microgrid architecture the with power-based control algorithm

some computational capability and with some sensing capability; specifically, they can sense the electrical quantities of interest (i.e., power and voltage magnitudes) at their point of connection within the electrical layer. Finally we assume that the master unit (i.e., the MC) can communicate with the slave units (i.e., the EGs) via a communication channel, which may be, for example, the same power lines (i.e., via power-line communication technologies).[1]

III. A MODEL-FREE POWER-BASED CONTROL STRATEGY

In this section we propose an algorithm which regulates the power injection of each EG so that:

- the power flow at the microgrid's PCC (i.e., the PCC power flow) follows a pre-assigned profile;
- the voltage magnitudes at the point of connection of the EGs are below a given threshold $U_{\max}$ (usually given as a percentage of the nominal voltage magnitude).

For the sake of clarity, only the control of the active power is considered in this paper. A similar approach can be employed also to regulate the reactive power injections from EGs, as outlined in [9].

We assume that each EG regulates the injection of active power every T seconds and we refer to the time interval $[(\ell - 1)T, \ell T]$ as the ℓ-th cycle of the control algorithm.

To the end of regulating the PCC power flow, the interaction among the MC and the EGs takes place in two phases. In the first phase, the master controller *gathers* from each EG a data packet that conveys the information of its local energy availability; in the second phase, the master controller *broadcasts* to all the EGs a common control packet that is finally translated by each EG into a particular power reference.[2] Fig. 2 shows the control steps composing the

algorithm.

In this paragraph, the details on how the proposed algorithm operates are explained more formally. For $h \in \{1, \ldots, m\}$, where m denotes the number of EGs in the microgrid, let EG_h denote the h-th EG. Then, for $h \in \{1, \ldots, m\}$, at the beginning of the $(\ell + 1)$-th cycle, that is, at time instant ℓT, EG_h sends a data packet to the master controller containing the following information:

- the measured active power $p_h(\ell T)$, namely, the active power injected by EG_h, at time instant ℓT; (For convenience quantities are denoted in the following simply by indicating the relevant control cycle, therefore, for example, by using $p_h(\ell)$ in place of $p_h(\ell T)$.)
- the estimated active power $\hat{p}_h(\ell + 1)$ that will be generated by the local renewable source in the current control cycle, namely, during the time interval $(\ell T, (\ell + 1)T)$—this estimate can be done on the basis of the status of the adopted renewable source (e.g., irradiation measurements for photovoltaic modules);
- the estimated minimum active power $\hat{p}_h^{\min}(\ell + 1)$ and maximum active power $\hat{p}_h^{\max}(\ell + 1)$ that the EG can inject during the current control cycle by taking into account all the local constraints, including the maximum power that can be delivered ($\hat{p}_{Sh}^{\text{out}}$) or absorbed ($\hat{p}_{Sh}^{\text{in}}$) by the local energy storage unit; in particular:
  - if $|u_h(\ell)| < U_{\max}$ (i.e., no voltage violations), then

$$\begin{cases} \hat{p}_h^{\min}(\ell + 1) = \hat{p}_h(\ell + 1) - \hat{p}_{Sh}^{\text{in}}(\ell + 1) \\ \hat{p}_h^{\max}(\ell + 1) = \hat{p}_h(\ell + 1) + \hat{p}_{Sh}^{\text{out}}(\ell + 1) \end{cases}, \quad (5)$$

  otherwise,
  - if $|u(\ell)| \geq U_{\max}$, which corresponds to an overvoltage condition at the point of connection of the h-th EG, then $\hat{p}_h^{\min}$, $\hat{p}_h^{\max}$ and $\hat{p}_h$ are set equal to $p_h(\ell)$, that is

$$\hat{p}_h^{\min}(\ell + 1) = \hat{p}_h^{\max}(\ell + 1) = \hat{p}_h(\ell + 1) := p_h(\ell). \quad (6)$$

[1]An investigation about the feasibility of such approaches in terms of the performance required to the communication channel is presented in [11], where the Long-Term Evolution (LTE) technology is addressed.

[2]It is worth remarking that to broadcast a single, unique, reference to *all* the controllable units represents an advantageous feature of the approach, because it limits the workload to the communication infrastructure.

Observe that in (5), $\hat{p}_h^{\min}$ and $\hat{p}_h^{\max}$ are computed assuming that all the power potentially available from the renewable source (i.e., $\hat{p}_h(\ell+1)$) is fully exploited, either by means of power injection into the grid or by recharging local storage devices. The rationale behind (6) will be clear later on, while explaining the algorithm proposed to control the microgrid.

Concurrently with the operation of the EGs, the master controller measures the power absorption $p_0(\ell)$ at microgrid's PCC, and receives the data packets form EGs. Then the MC calculates the overall parameters p_{tot}, $\hat{p}_{tot}$, $\hat{p}_{tot}^{\min}$, $\hat{p}_{tot}^{\max}$ for the entire microgrid:

$$p_{tot}(\ell) = \sum_h p_h(\ell)$$
$$\hat{p}_{tot}(\ell+1) = \sum_h \hat{p}_h(\ell+1)$$
$$\hat{p}_{tot}^{\min}(\ell+1) = \sum_h \hat{p}_h^{\min}(\ell+1)$$
$$\hat{p}_{tot}^{\max}(\ell+1) = \sum_h \hat{p}_h^{\max}(\ell+1). \tag{7}$$

and estimates the total load of the microgrid as:

$$p_L(\ell) = p_0(\ell) + p_{tot}(\ell), \tag{8}$$

which takes into account comprehensively the overall electrical load and the losses on the power lines. Finally, given a pre-assigned power profile p_0^* at the PCC of the microgrid,[3] the MC estimates the total power that the set of EGs have to provide during the $(\ell+1)$-th cycle:

$$p_{tot}^*(\ell+1) = p_L(\ell) - p_0^*(\ell+1). \tag{9}$$

On the basis of the quantities reported above, the MC computes a coefficient that is broadcasted to all the EGs. This coefficient, here indicated as α_p for active power control, conveys the information on the global status of the microgrid in terms of the required power with respect to the available power from EGs. Specifically, the coefficient α_p takes values as follows.

- If $p_{tot}^*(\ell+1) < \hat{p}_{tot}^{\min}(\ell+1)$ then:

$$\alpha_p = 0; \tag{10}$$

  in this case, the loads are expected to absorb a total active power lower than the minimum power the active nodes can deliver. The overproduction is exported to the main grid.
- If $\hat{p}_{tot}^{\min}(\ell+1) \leq p_{tot}^*(\ell+1) < \hat{p}_{tot}(\ell+1)$ then:

$$\alpha_p = \frac{p_{tot}^*(\ell+1) - \hat{p}_{tot}^{\min}(\ell+1)}{\hat{p}_{tot}(\ell+1) - \hat{p}_{tot}^{\min}(\ell+1)}; \tag{11}$$

  in this case the expected load power is lower than the generated power but the excess of generation can be diverted into distributed storage units.

- If $\hat{p}_{tot}(\ell+1) \leq p_{tot}^*(\ell+1) \leq \hat{p}_{tot}^{\max}(\ell+1)$ then:

$$\alpha_p = 1 + \frac{p_{tot}^*(\ell+1) - \hat{p}_{tot}(\ell+1)}{\hat{p}_{tot}^{\max}(\ell+1) - \hat{p}_{tot}(\ell+1)}; \tag{12}$$

  in this case the expected load power is higher than generated power but the difference can be supported by distributed energy storage.
- If $p_{tot}^*(\ell+1) > \hat{p}_{tot}^{\max}(\ell+1)$ then:

$$\alpha_p = 2; \tag{13}$$

  in this case the loads are expected to absorb a total power which is greater than the maximum power the active nodes can deliver. The power deficiency will be imported from the main grid.

Finally, once a new coefficient α_p is available, for $h \in \{1, \ldots, m\}$, EG_h determines the power to be injected as:

$$\begin{aligned} p_h^* = &\; \hat{p}_h^{\min}(\ell+1) + \\ &+ \left(\hat{p}_h(\ell+1) - \hat{p}_h^{\min}(\ell+1)\right) \cdot \min\left(\alpha_p, 1\right) + \\ &+ \left(\hat{p}_h^{\max}(\ell+1) - \hat{p}_h(\ell+1)\right) \cdot \max\left(\alpha_p - 1, 0\right). \end{aligned} \tag{14}$$

The control principle behind (14) is to make EGs to contribute to microgrid power needs—measured at the microgrid's PCC—in proportion of their *capability* of deliver or absorb power, thus allowing to obtain a uniform exploitation of available resources, without preventing EGs to pursue local objectives.

Assuming that all the transmissions and computations performed by the MC and the EGs take a negligible amount of time with respect to T, then EG_h injects the power p_h^* right after the instant ℓT, namely:

$$p_h\left(\ell T^+\right) = p_h^*, \tag{15}$$

where ℓT^+ denotes the time instant just after ℓT.

In order to maintain the voltage magnitude below a given threshold $U_{\max}$ within the interval $(\ell T, (\ell+1)T)$, for $h \in \{1, \ldots, m\}$, EG_h applies a voltage control which is based only on local measurements of the voltage magnitude. Precisely, EG_h continuously measures $|u_h|$ and, in case an overvoltage[4] occurs at some time instant $\bar{t} \in (\ell T, (\ell+1)T)$, it adjusts the power injection according to the following rule:

$$\dot{p}_h(t) = -k\left(|u_h(t)| - U_{\max}\right). \tag{16}$$

for $t \geq \bar{t}$, where $p_h(\bar{t}) = p_h^*$.[5] We assume that in this case EG_h keeps applying the *purely local voltage control* described in (16) within all the interval $(\bar{t}, (\ell+1)T)$.

Observe that, if at time instant $(\ell+1)T$, EG_h is still in overvoltage condition (i.e., $|u_h(t)| \geq U_{\max}$), then, according to (6), EG_h will set $\hat{p}_h^{\min}(\ell+2) = \hat{p}_h^{\max}(\ell+2) = p_h\left((\ell+1)T\right)$, thus implying, from (14), that

[3]From a practical standpoint, p_0 is negotiated with the distribution system operator and set to obtain the higher economic benefit for the microgrid; a choice that is technically convenient is, for example, to set p_0^* constant and equal to the expected mean power absorption at the microgrid PCC.

[4]An overvoltage can be due to different reasons, like, for example, increase of production from renewable sources, disconnection of large loads, connection of new generators, voltage magnitude adjustments by the distribution system operator.

[5]The effectiveness of controlling the active power injections to regulate node voltage magnitudes is discussed in Remark 4.

$p_h\left((\ell+1)T^+\right) = p_h\left((\ell+1)T\right)$; in other words the value of α_P sent from the MC at time instant $(\ell+1)T$ does not affect the power injection of EG_h, which, since it is still in overvoltage condition, will keep applying the rule (16) also during the $(\ell+2)$-th cycle of the algorithm.

Instead, if no overvoltage occurs, then EG_h continues to inject p_h^*, namely, $p_h(t) = p_h^*$ for all $t \in (\ell T, (\ell+1)T)$.

The rationale behind this local control law is the following. If the node at which EG_h is connected is experiencing an overvoltage it means that node h cannot accept the power EG_h is injecting; accordingly, EG_h starts to decrease p_h as described in (16), relaying on the fact that in a mainly resistive scenario, by decreasing the active power injection at grid nodes, the corresponding voltage magnitudes decrease as well. We will make more formal this reasoning in the following section.

Observe also that, if there exists $\tilde{t}$ such that $\left|u\left(\tilde{t}\right)\right| = U_{\max}$, then the power $p_h(\tilde{t})$ represents the power that the node where EG_h is connected can receive without experiencing overvoltages. In general, it might happen that, during the overvoltage condition, $\hat{p}_h\left((\ell+1)T\right) < \hat{p}_h^{\min}(\ell+1)$; in this case the overproduction $\hat{p}_h^{\min}(\ell+1) - \hat{p}_h\left((\ell+1)T\right)$ is assumed to be curtailed.

Next, we provide a compact algorithmic description of the proposed control.

ALGORITHM 1

Let's consider the $(\ell+1)$-th cycle. The following actions take place in order:

1. Each EG_h sends $p_h(\ell)$, $\hat{p}_h(\ell+1)$, $\hat{p}_h^{\min}(\ell+1)$, $\hat{p}_h^{\max}(\ell+1)$.
2. On the basis of the received data, MC computes quantities (7), (8), and (9).
3. The MC computes and broadcasts to all the EGs the new value of α_p.
4. Each EG computes—by using (14)—and actuates its power reference p_h^*.

For all the duration of the cycle, EG_h keeps on measuring $|u_h|$ and if an overvoltage condition is detected then the local control rule (16) is applied.

Some remarks are now reported in order.

Remark 1: Observe that both the MC and the EGs have no knowledge of the network's model, namely, the algorithm is *model free*.

Remark 2: It is worth remarking that, while quantity p_h can be directly measured, quantities $\hat{p}_h$, $\hat{p}_h^{\max}$, and $\hat{p}_h^{\min}$ have to be locally estimated. The estimation of $\hat{p}_h$ can be done on the basis of the status of the adopted renewable source (e.g., irradiation measurements for photovoltaic modules); the estimate of $\hat{p}_h^{\max}$, and $\hat{p}_h^{\min}$, on the other hand, can be obtain by considering the state of charge of the local storage device, as indicated in (5), or to accommodate particular needs of the EG, by employing predictive models and statistical information.

Remark 3: From a practical point of view, the electronic power processors are assumed to be controlled as current sources, in compliance with current grid connection standards [12]. However, the proposed architecture is suitable and all the considerations are valid also if electronic power processors are controlled as voltage sources (droop-like control).

Remark 4: The use of reactive power capabilities of DERs to control voltage profiles, which does not virtually involve additional costs, has been shown to be an effective and advantageous solution in medium-voltage (MV) networks [13], where interconnection impedances are mainly inductive (i.e., characterized by low R/X ratios). However, this approach is not adequate in low-voltage networks, where, instead, interconnection impedances are typically resistive (i.e., R/X ratios are high) [14], [15]. Indeed, in networks with high R/X ratios, the reactive power injection that would be needed to counteract voltage rises caused by excessive active power injections may be so intense to lead to detrimental effects on the electrical infrastructure (e.g., overload of MV/LV transformer and distribution cables) and affect EPPs reliability [16]. Therefore, approaches based on active power control are more suitable in high R/X microgrids, with the main drawback of the potential reduction in the overall power production, which, though, can be alleviated or even eliminated with small local accumulation.

Remark 5: One of the advantages given by distributed generation (with devices installed, ideally, at the consumers' premises) is to generate the active power closer to the loads, namely, to the point where it is consumed. This helps in compensating the voltage drops that would be naturally present due to the active power absorption by loads [8]. In addition, the control proposed herein coordinate the power injection by DERs so that it can adapt to the need of the microgrid's loads and to share the load among the generators in a fair way (specifically, according to their power availability). This contributes in sustaining the grid voltage to avoid *undervoltage* conditions. On the other hand, *overvoltages* are an intrinsic issue of distributed generation in low-voltage grids. Indeed, overvoltages may occur due to congestion of distribution lines during periods of peak production from renewables, or can rise due to an excessive power injection by one or more distributed resources (e.g., in response to a remote control signal, like the one here referred to as α_p). These particular aspects, instead, are dealt with the local overvoltage control technique.

IV. ANALYSIS OF THE PROPOSED ALGORITHM

In this section we characterize the main features of Algorithm I. In particular we are interested into:

- *purely local* properties, namely, the effectiveness of the rule in (16);
- *global* properties, namely, the ability to track the pre-assigned profile p_0^*, while satisfying the loads' requests and solving possible overvoltage situations.

Since the control algorithm can be performed on a very fast time scale, we assume that all the uncontrolled system variables, in particular, the power absorbed by the loads, the pre-assigned power profile p_0^*, and the predicted quantities $\hat{p}_{tot}$, $\hat{p}_{tot}^{\min}$, $\hat{p}_{tot}^{\max}$, remain constant. Formally, we make the following assumption.

Assumption 1: Let p_0^*, p_L, $\hat{p}_{tot}$, $\hat{p}_{tot}^{\min}$ and $\hat{p}_{tot}^{\max}$ be defined as in the previous Section III. Then:

$$p_0^*(\ell) = c_1, \ \ p_L(\ell) = c_2, \ \ \hat{p}_{tot}(\ell) = c_3$$
$$\hat{p}_{tot}^{\min} = c_4, \ \ \hat{p}_{tot}^{\max} = c_5,$$

where c_1, c_2, c_3, c_4, c_5 are suitable constants.

Before proceeding with the analysis of the purely local and global properties separately, it is useful to introduce a suitable approximated model for the distribution grid. In the scenario considered herein, where distribution lines are mainly resistive, we can approximate the relation between voltage magnitudes and power injections via:

$$|u| = \frac{1}{U_N}\Re X p + \mathbf{1} U_N + o\left(\frac{1}{U_N}\right) \tag{17}$$

where the little-o notation means that $\lim_{U_N \to \infty} \frac{o(f(U_N))}{f(U_N)} = 0$ and where, with a slight abuse of notation, $|u|$ indicates the vector obtained stacking all the voltages' magnitudes $|u_h|$, $h \in V$.

The above approximation follows from the model developed in [10]. The quality of this approximation relies on having large nominal voltage U_N and relatively small currents injected by the inverters (or supplied to the loads). This assumption is verified in practice, and corresponds to correct design and operation of power distribution networks, where indeed the nominal voltage is chosen sufficiently large (subject to other functional constraints) in order to deliver electric power to the loads with relatively small power losses on the power lines.

The results reported in the following two subsections are obtained neglecting the infinitesimal term in (17) (i.e., assuming $\bar{u}| = \frac{1}{U_N}\Re X p + \mathbf{1} U_N$).

A. Purely local properties

Consider the ℓ-th cycle of Algorithm I. Let us collect in the sets $\mathcal{L}$, $\mathcal{H}$, and $\mathcal{K}$, respectively, the uncontrolled nodes, the EGs experiencing an overvoltage, and the EGs not experiencing an overvoltage. It is convenient to partition the variables describing the system state by grouping together the nodes belonging to the same set; doing so, as far as the voltages are concerned, we can write:

$$u = \begin{bmatrix} u_0 & u_{\mathcal{L}}^T & u_{\mathcal{H}}^T & u_{\mathcal{K}}^T \end{bmatrix}^T.$$

Clearly, similar partitions hold also for the other electrical quantities.

Now, by decomposing the Green matrix X according to the former partitioning, from (17), it follows that:

$$|u_{\mathcal{H}}| = \frac{1}{U_N}\big(\Re(X_{\mathcal{H}\mathcal{L}})p_{\mathcal{L}} + \Re(X_{\mathcal{H}\mathcal{K}})p_{\mathcal{K}} + \Re(X_{\mathcal{H}\mathcal{H}})p_{\mathcal{H}}\big) + \mathbf{1} U_N$$

Recall that the EGs belonging to $\mathcal{H}$ perform, during the interval $((\ell-1)T, \ell T)$, the local control given by (16), which, exploiting the above equation, can be rewritten as:

$$\dot{p}_{\mathcal{H}} = -\frac{k}{U_N}\Re(X_{\mathcal{H}\mathcal{H}})p_{\mathcal{H}} - \frac{k}{U_N}\big(\Re(X_{\mathcal{H}\mathcal{L}})p_{\mathcal{L}} + \Re(X_{\mathcal{H}\mathcal{K}})p_{\mathcal{K}}\big)$$
$$- k\mathbf{1}(U_N - U_{\max}). \tag{18}$$

Notice that, being $|u_{\mathcal{H}}| \geq U_{\max}$, the effect of the local control action is to decrease the power injected by the nodes in $\mathcal{H}$. Since $\Re(X_{\mathcal{H}\mathcal{H}})$ is a real, symmetric, positive definite matrix, its eigenvalues are all positive real numbers and thus the dynamic system ruled by (18) is asymptotically stable. Therefore the local controller drives the system toward the equilibrium of (18), which, by straightforward computations, turns out to be:

$$p_{\mathcal{H}}^* = -\Re(X_{\mathcal{H}\mathcal{H}})^{-1}\big(\Re(X_{\mathcal{H}\mathcal{L}})p_{\mathcal{L}} + \Re(X_{\mathcal{H}\mathcal{K}})p_{\mathcal{K}} + \mathbf{1} U_N(U_N - U_{\max})\big). \tag{19}$$

By substituting $p_{\mathcal{H}}^*$ in (18), one can see that $p_{\mathcal{H}}^*$ amounts to the power injection for which $|u_{\mathcal{H}}| = U_{\max}$; namely, the local control in (16) drives the voltages' magnitudes of the EGs experiencing an overvoltage toward $U_{\max}$.

B. Global properties

In this subsection, in addition to Assumption 1, we assume that the dynamics of the local control in (16) are completed within the cycle in which they are activated. Specifically this is equivalent to assume the following property.

Assumption 2: Consider the ℓ-th cycle of Algorithm I and let $\mathcal{H}$ be the subset of EGs which experience an overvoltage condition within $((\ell - 1)T, \ell T)$. Let node h belong to $\mathcal{H}$. Then $|u(\ell T)| = U_{\max}$.

The global properties of the proposed algorithm are established in the following proposition.

Proposition 1: Consider Algorithm I. Assume Assumptions 1 and 2 hold true. Consider the sequence $\{\alpha_p(\ell)\}$ generated by the MC. Then there exist a value $\bar{\alpha}_p \in [0, 2]$ such that:

$$\lim_{\ell \to \infty} \alpha_p(\ell) = \bar{\alpha}_p.$$

In addition, if $\bar{\alpha} \in (0, 2)$, then:

$$\lim_{\ell \to \infty} p_0(\ell) = p_0^*.$$

Observe that the cases $\bar{\alpha} = 0$ and $\bar{\alpha} = 2$ might happen when, respectively, $p_{tot}^*(\ell + 1) < \hat{p}_{tot}^{\min}$ and $p_{tot}^*(\ell + 1) > \hat{p}_{tot}^{\max}$. In general, in both these situations, we cannot have $\lim_{\ell \to \infty} p_0(\ell) = p_0^*$.

Remark 6: The assumption 2 might be not always realistic, though, the local control law (16) can be designed to be conveniently fast to have $|u_h| \approx U_{\max}$. Besides, in the numerical section, we show the effectiveness of the overall algorithm in obtaining the results stated in Proposition 1.

Legend:

- •   load
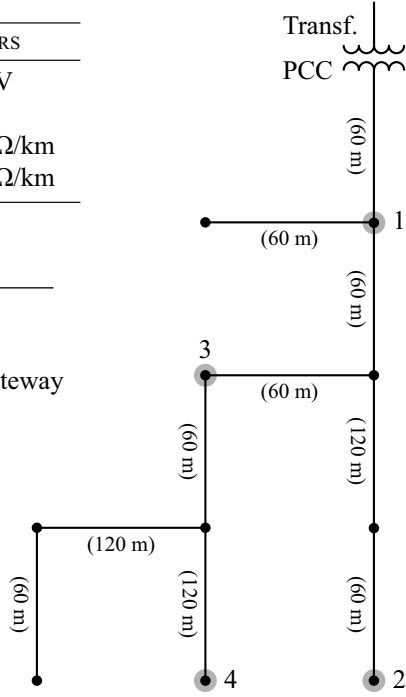- ⊙   energy gateway
- $\overline{(length)}$ line

Fig. 4.   Low-voltage distribution

V. SIMULATIONS

In this section, we simulate Algorithm I on a realistic low-voltage network, sketched in Fig. 4. It represents an actual distribution grid located in Brazil. The network interconnects ten nodes, which represent ten houses. Four of them are equipped with an EG (see Fig. 3) and a load, while the others behave like passive loads. The MC gathers the data from the EGs and sends them back the coefficient α_p every $T = 5$ seconds, while the EGs measure their voltage magnitude every 0.1 s and possibly perform the local voltage control.

Clearly the simulation testbed does not satisfy the simplifying assumptions we made for the algorithm description (e.g., the linear relation between voltages' magnitudes and powers), being the electrical grid a highly non-linear system. In spite of that, Fig. 5, Fig. 6, Fig. 7, and Fig. 8 show the effectiveness of the proposed algorithm also in this realistic scenario.

In Fig. 5 and in Fig. 6, we depict, respectively, the trajectories of the voltage magnitudes and of the amounts of power injected. Notice, in Fig. 5, that EG_2 and EG_4 experience several overvoltage situations but, at the steady state, the local control law drives their voltage magnitudes on the admissible limit. As a consequence, EG_2 and EG_4 decrease the amounts of power they inject into the grid, i.e, p_2 and p_4; in turn, in order to meet the requirement of p_0^*, EG_1 and EG_3 increase p_1 and p_3, see Fig. 6.

The behavior of the power flow at the PCC is reported in Fig. 7. We can see that p_0 tends to the desired value p_0^*.

Finally, in Fig. 8 we report the values of the sequence $\alpha(\ell)$ generated by the MC; we can see that $\alpha(\ell)$ converges to a limit value $\bar{\alpha}_p$ as predicted in Proposition 1.
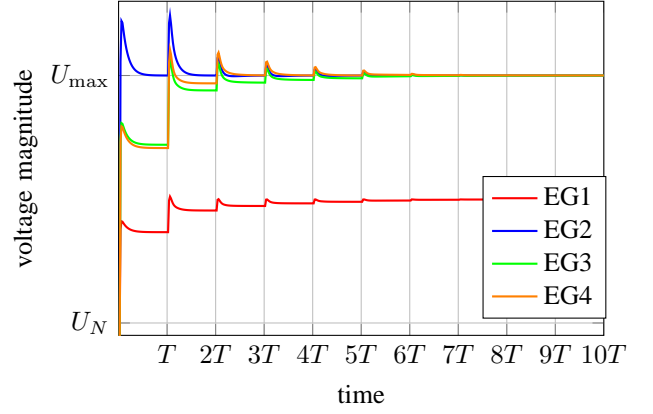

Fig. 5.   Voltage magnitude of the EGs
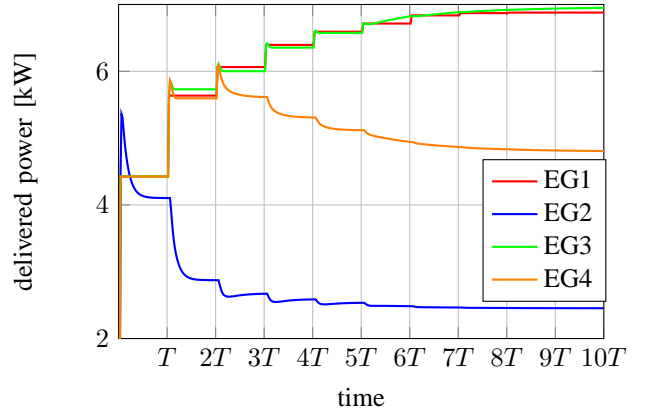

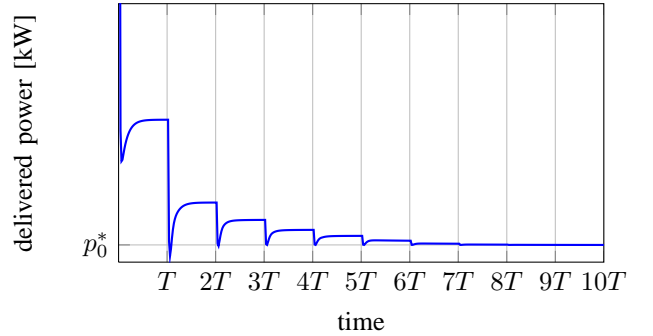Fig. 6.   Power injected by the EGs
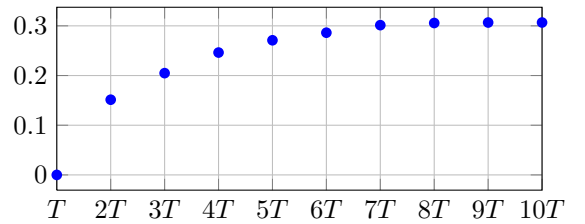

Fig. 7.   Power flowing through the PCC

Fig. 8.   Sequence of values assumed by coefficient α_p

VI. Conclusion

A simple approach to the synergistic control of distributed energy resources in low-voltage microgrids was presented and analyzed. It only requires non-time-critical power data to be transferred from the active nodes to a centralized controller through a narrowband communication link. The centralized controller, in turn, broadcasts active power set-points for all the active nodes.

The control of the power flow (taking place centrally, at microgrid PCC) and the local overvoltage control (performed distributedly, at each EG) cooperate so that both the power flow at microgrid PCC and the voltage magnitudes at the point of connection of EGs can be simultaneously regulated.

The controller was tested by simulations referring to a realistic application scenario. The results have shown that the centralized power-based control strategy succeed in controlling the active power exchanged at PCC and avoids local overvoltages.

Appendix

The proof of Proposition 1 exploits the property stated in the following lemma.

Lemma 1: Let h be an EG such that $|u(\ell^+)| > U_{\max}$, i.e. h is experiencing an overvoltage after the active power injection regulated by the coefficient α_p computed by the MC in the ℓ-th control cycle. Let Assumption 1 and 2 hold true. Then, $|u_h(\ell + 1^+)| > U_{\max}$, i.e. h's voltage will be greater than $U_{\max}$ also after the next MC action.

Proof: Let h be an EG such that $|u_h(\ell^+)| \geq U_{\max}$, i.e.

$$|u_h(\ell^+)| = \sum_{k \in H} \frac{\Re(X_{hk})}{U_N} p_k(\ell^+) + \sum_{k \in G} \frac{\Re(X_{hk})}{U_N} p_k(\ell^+) + \mathbf{1} U_N \geq U_{\max}.$$

During the interval $(\ell T, (\ell + 1)T)$ the local controllers act on the power injected by the EGs in H by decreasing them until $p_H(\ell + 1)$, such that $|u_H| = \mathbf{1} U_{\max}$, i.e.,

$$|u_h(\ell + 1)| = \sum_{k \in G} \frac{\Re(X_{hk})}{U_N} p_k(\ell + 1)$$
$$+ \sum_{k \in H} \frac{\Re(X_{hk})}{U_N} p_k(\ell^+) + \mathbf{1} U_N = U_{\max}. \quad (20)$$

The $p_H(\ell + 1)$ are then sent to the MC, for the computation of the new coefficient α_P. Notice that the total amount of power generated by the EGs at time $(\ell + 1)T$, i.e. before the master control action, is lower than the amount that should be generated in order to guarantee the meet of the pre-assigned power profile p_0^*, and thus the master controller will act in order to increase the power genneration. On the other hand, the power reference for the node in H will remain $p_H(\ell+1)$, and thus the generation increase will be entrusted to EGs in G, i.e. $p_h(\ell + 1^+) > p_h(\ell^+), h \in G$. The nodes in H will experience again the overvoltage, since

$$|u_h(\ell + 1^+)| = \sum_{k \in G} \frac{\Re(X_{hk})}{U_N} p_k(\ell + 1^+) + \mathbf{1} U_N$$
$$+ \sum_{k \in H} \frac{\Re(X_{hk})}{U_N} p_k(\ell + 1) > U_{\max}. \quad (21)$$

$\blacksquare$

Proof: [Proof of Proposition 1] Consider a run of the control algorithm. For $\ell = 1$, once the master control receives the parameters defined in (7), it computes and broadcasts to the EGs $\alpha_p(1)$. Then, EGs inject $p(1^+)$. After that, the nodes belonging to H decrease the power injected until $p_H(2)$, which is, for Assumption 2, such that $|u_h(2)| = U_{\max}$, and set all their parameters equal to $p_H(2)$, as in equation (6).

Let us define $\Delta_h(\ell) = p_h(\ell^+) - p_h(\ell + 1), h \in H$, and $\Delta(\ell) = \sum_{h \in H} \Delta_h(\ell)$. A consequence of Lemma 1 is that the nodes in H keep to decrease the power they inject and the references they send to the master controller. Thus, $\Delta_h(\ell)$ is always greater than zero and furthermore $p_h(\ell + 1), \hat{p}_h(\ell + 2), \hat{p}_h^{\min}(\ell + 2), \hat{p}_h^{\max}(\ell + 2)$ will be always lower than $p_h(\ell), \hat{p}_h(\ell + 1), \hat{p}_h^{\min}(\ell + 1), \hat{p}_h^{\max}(\ell + 1)$, respectively, $\forall \ell \geq 2$.

In particular, it is easy to verify that, for $\ell \geq 3$

$$\alpha_p(\ell) = \left[\frac{p_{tot}^* - \hat{p}_{tot}^{\min}(\ell + 1)}{\hat{p}_{tot}(\ell + 1) - \hat{p}_{tot}^{\min}(\ell + 1)} \right]_0^1$$
$$+ \left[\frac{p_{tot}^* - \hat{p}_{tot}(\ell + 1)}{\hat{p}_{tot}^{\max}(\ell + 1) - \hat{p}_{tot}(\ell + 1)} \right]_0^1$$
$$\geq \alpha_p(\ell - 1)$$

and thus the sequence $\{\alpha(\ell)\}_{\ell \geq 3}$ is a non decreasing sequence. Since $\alpha(\ell)$ is always lower than 2, there exists a $\bar{\alpha}_p$ such that

$$\lim_{\ell \to \infty} \alpha_p(t) = \bar{\alpha}_p$$

When $\bar{\alpha}_p \in (0, 2)$ we have two cases:

1) the case in which $\alpha_p \in (0, 1]$, and thus

$$\bar{\alpha}_p = \frac{p_{tot}^* - \hat{p}_{tot}^{\min}}{\hat{p}_{tot} - \hat{p}_{tot}^{\min}}$$

2) the case in which $\alpha_p \in (1, 2)$,

$$\bar{\alpha}_p = 1 + \frac{p_{tot}^* - \hat{p}_{tot}}{\hat{p}_{tot}^{\max} - \hat{p}_{tot}}.$$

In both the cases, by substituting $\tilde{\alpha}_p$ in (14) and by adding the contribute of every EG, we obtain that the power delivered by the EGs is exactly p_{tot}^* and thus both the pre-assigned value p_0^* and the power demand are satisfied. Furthermore, the fact that $\{\alpha_p(\ell)\}$ converges to $\bar{\alpha}_p$ implies that both the sequences $\{\hat{p}_{tot}^{\min}(\ell)\}$ and $\{\hat{p}_{tot}^{\max}(\ell)\}$ converges to a final value. This implies that, in the end, the local controllers do not act anymore, and thus that $|u_h| \leq U_{\max}$, for every EG h. $\blacksquare$

References

[1] S. Parhizi, H. Lotfi, A. Khodaei, and S. Bahramirad, "State of the Art in Research on Microgrids: A Review," *IEEE Access*, vol. 3, pp. 890–925, 2015.

[2] IEA, "Overcoming PV grid issues in the urban areas," IEA International Energy Agency, Tech. Rep. IEA-PVPS T10-06-2009, 2009.

[3] F. Katiraei and J. Agüero, "Solar PV Integration Challenges," *IEEE Power and Energy Magazine*, vol. 9, no. 3, pp. 62–71, May 2011.

[4] ——, "Solar pv integration challenges," *IEEE Power and Energy Magazine*, vol. 9, no. 3, pp. 62–71, May 2011.

[5] J. M. Guerrero, J. C. Vasquez, J. Matas, L. G. de Vicuna, and M. Castilla, "Hierarchical Control of Droop-Controlled AC and DC Microgrids - A General Approach Toward Standardization," *IEEE Transactions on Industrial Electronics*, vol. 58, no. 1, pp. 158–172, 2011.

[6] J. Simpson-Porco, Q. Shafiee, F. Dorfler, J. Vasquez, J. Guerrero, and F. Bullo, "Secondary frequency and voltage control of islanded microgrids via distributed averaging," *Industrial Electronics, IEEE Transactions on*, vol. 62, no. 11, pp. 7025–7038, Nov 2015.

[7] J. Schiffer, T. Seel, J. Raisch, and T. Sezi, "Voltage stability and reactive power sharing in inverter-based microgrids with consensus-based distributed voltage control," *Control Systems Technology, IEEE Transactions on*, vol. PP, no. 99, pp. 1–1, 2015.

[8] P. Tenti, A. Costabeber, P. Mattavelli, and D. Trombetti, "Distribution Loss Minimization by Token Ring Control of Power Electronic Interfaces in Residential Microgrids," *IEEE Transactions on Industrial Electronics*, vol. 59, no. 10, pp. 3817–3826, Oct 2012.

[9] T. Caldognetto, S. Buso, P. Tenti, and D. Brandao, "Power-Based Control of Low-Voltage Microgrids," *IEEE Journal of Emerging and Selected Topics in Power Electronics*, vol. PP, no. 99, pp. 1–1, 2015.

[10] S. Bolognani and S. Zampieri, "A Distributed Control Strategy for Reactive Power Compensation in Smart Microgrids," *IEEE Transactions on Automatic Control*, vol. 58, no. 11, pp. 2818–2833, 2013.

[11] A. Angioni, A. Sadu, F. Ponci, A. Monti, D. Patel, F. Williams, D. Della Giustina, and A. Dede, "Coordinated voltage control in distribution grids with LTE based communication infrastructure," in *IEEE 15th International Conference on Environment and Electrical Engineering (EEEIC)*, June 2015, pp. 2090–2095.

[12] "Ieee standard for interconnecting distributed resources with electric power systems," *IEEE Std 1547-2003*, pp. 1–28, 2003.

[13] P. Carvalho, P. F. Correia, and L. Ferreira, "Distributed reactive power generation control for voltage rise mitigation in distribution networks," *IEEE Transactions on Power Systems*, vol. 23, no. 2, pp. 766–772, May 2008.

[14] R. Tonkoski, L. Lopes, and T. El-Fouly, "Coordinated Active Power Curtailment of Grid Connected PV Inverters for Overvoltage Prevention," *IEEE Transactions on Sustainable Energy*, vol. 2, no. 2, pp. 139–147, April 2011.

[15] M. Kabir, Y. Mishra, G. Ledwich, Z. Dong, and K. Wong, "Coordinated Control of Grid-Connected Photovoltaic Reactive Power and Battery Energy Storage Systems to Improve the Voltage Profile of a Residential Distribution Feeder," *IEEE Transactions on Industrial Informatics*, vol. 10, no. 2, pp. 967–977, May 2014.

[16] A. Anurag, Y. Yang, and F. Blaabjerg, "Thermal Performance and Reliability Analysis of Single-Phase PV Inverters with Reactive Power Injection Outside Feed-In Operating Hours," *IEEE Journal of Emerging and Selected Topics in Power Electronics*, vol. in press, 2015.